# Green Chemistry

Accepted Manuscript






ROYAL SOCIETY OF CHEMISTRY

www.rsc.org/greenchem

ARTICLE TYPE www. rsc.org/xxxxxx | XXXXXXXX

# A Theoretical Study of the Nornicotine-Catalyzed Mannich Reaction in Wet Solvents and Water†

**Sheng-Che Yang‡, Timm Lankau‡ and Chin-Hui Yu***

*Received Xth XXXXXXXXXX 20XX, Accepted Xth XXXXXXXXX 20XX*
*First published on the web Xth XXXXXXXXXX 200X*
**DOI: 10.1039/b000000x**

Nornicotine can catalyze the intermolecular Mannich reaction in wet solvents and water to enable a green version of this versatile C–C bond forming reaction. M06-2X/6-31++G(d,p) calculations combined with a polarizable continuum model are used to explore the possibilities of nornicotine catalysis. The bottleneck of the uncatalysed Mannich reaction is the formation of the enol from the ketone, while the catalysed reaction is hindered by the formation of the enamine from the ketone and nornicotine. The calculated barriers for the enamine formation are significantly lower than those for the enol formation and an overall speed-up of the Mannich reaction predicted. The detailed analysis of four possible reaction paths suggests that nornicotine has a mild stereoinductive effect onto the Mannich reaction favoring the *S*-Mannich product. The analysis further shows that water molecules play an active role in the reaction and indicates that solvents actually need to be wet for nornicotine catalysis.

## 1 Introduction

The Mannich reaction is an important reaction for the consecutive formation of C–N and C–C bonds yielding $\beta$-aminocarbonyl compounds (Mannich bases), and it is frequently applied in the synthesis[1,2] of pharmaceuticals and natural products. Volatile organic compounds such as benzene, THF, acetone and DMSO are common solvents in these procedures.[3,4] Water is usually regarded as a contaminant and has to be chemically removed to prevent the hydrolysis of the intermediate imines. Using wet solvents or water to avoid the costly and potentially hazardous dehydration would make the Mannich reaction as well as syntheses of many organic compounds much greener.[5–8]

Significant parts of biochemistry and clinical chemistry are in fact organic reactions in water; thus, biochemistry provides a good starting point for the design of water-based synthetic procedures. An efficient catalyst readily available from a natural feedstock rather than from extended chemical synthesis fits even better into the concept of green chemistry. Nornicotine is formed from nicotine in the tobacco plant *Nicotiana tabacum*[9–12] and is part of the pathogenesis of smoking-related diseases.[13,14] Nornicotine is also known to catalyze the aldol reaction in aqueous media as shown by Janda *et al.*[15–17] Crucial for pathogenesis and aldol reaction are water-stable enamines and related compounds derived from nornicotine.[17]

Enzymicatic catalysis is frequently regarded as critical to biochemical synthesis under physiological conditions. Carl Mannich was among the first to ask whether the synthesis of complex compounds such as alkaloids is possible without enzymes. Schöpf *et al.* answered this question with the successful synthesis of several alkaloids[18,19] under physiological conditions: pH buffer close to 7, room temperature, and dilute solution of the reactants. The reactants chosen by Schöpf *et al.* reveal that an intramolecular Mannich-type reaction plays a central role in those reactions. Of special interest is the reaction of tryptamine with ethanal yielding tetrahydroharman where the RNH–CH=$CR_2$ motif in tryptamine can be regarded as the enamine analogon of the enol in a Mannich reaction. Enamines as substitutes for enols in Mannich reactions were also reported by Esser and Risch, who used benzene as the solvent for the synthesis of enamines which are water and air sensitive.[3,20] The imine in their version of the Mannich reaction has been replaced by an imminium tetrachloroaluminate, which is sufficiently reactive at low temperatures and is relatively easy to handle.

Enantioselective Mannich reactions catalysed by small organic molecules with high yields in solvents containing various amounts of water have been reported.[4,21–27] The majority of these studies uses functionalised proline derivatives as catalysts with the notable exception of Cheng *et al.* who use threonine derivatives.[25] An enamine based mechanism[22,25] has been proposed for these reactions in which the catalyst forms an enamine with the ketone which is an ex-

* *Department of Chemistry, National Tsing Hua University, 30013 Hsinchu, Taiwan. Fax: +886-3-5711082; Tel: +886-3-5162080; E-mail: chyu@oxygen.chem.nthu.edu.tw*
‡ These authors contributed equally to this work.
† Electronic Supplementary Information (ESI) available: Test of the DFT functionals; reaction path for the rotation of the cyclohexene ring in the nornicotine-derived enamine; complete ref. 26; the Cartesian coordinates, the six lowest frequencies and Mulliken atomic charges of the optimized stationary points; frequency and energy data for the alcohols; molecular dynamics results. See DOI: 10.1039/b000000x/

cellent reaction partners for imines.[1,3,20] However, proline-derived enamines are unstable in water and hydrolyze quickly under physiological condition.[15] Mannich reactions catalysed by proline require $H_2O$/THF mixtures as solvents[21] with mixing ratios varying between 1/9 and 1/1. Hayashi *et al.* further reported that proline fails to catalyse the Mannich reaction in pure water.[26] Large and hydrophobic substituents such as *tert*-butyldiphenylsilyloxy[25,26] and diphenyl(trimethylsilyl)methyl group[23] appear to be a prerequisite for proline catalysis in water. In contrast, the experimental and theoretical analysis of the similar nornicotine catalyzed aldol reaction showed that water molecules actually play an active role as proton shuttles in the mechanism of the enamine based catalysis.[28–30]

Another water sensitive element in the Mannich reaction is the imine. Lehn *et al.* proposed a method to evaluate the stability of imines in water which can be used to select suitable reactants.[31] A recent study also suggests that surfactants can increase the yield of imines in water.[32] An acidic catalyst, on the other hand, accelerates the decay of the imine leading to a poor overall yield of the Mannich reaction.[26]

Nornicotine forms water stable enamines, has no acidic protons and the data for the aldol reaction show that no substitution is necessary to work in water. Moreover, its water solubility and an octanol-water partition coefficient[33] $\log P$ of 0.17 reveal that nornicotine can be retrieved from the organic product by a simple extraction with water. We investigate the feasibility of a green version of an intermolecular Mannich reaction in wet and aqueous solvents by computational simulation in this study. The reminder of the paper is organized as follows: The computational details are described in the next section. Results and discussions are combined in section three. Its first subsection focuses on the original Mannich reaction to serve as the reference. It is followed by the discussion of the imine hydrolysis, the formation of the nornicotine-derived enamine, the possible stereoselectivity of the catalyst nornicotine, and the release of the Mannich base, squencially. The final subsection focuses on the effect of different solvents onto the catalytic cycle. Finally, conclusions are summarized in section four.

## 2 Computational Details

The Gaussian 09 program package[34] was used for all calculations. The geometries, energies, charges and frequencies of selected structures are listed in the ESI†. Truhlar's hybrid meta exchange-correlation functional M06-2X[35] and the 6-31++G(d,p) basis set were used for all calculations presented herein.[36–39]

A benchmark paper by Truhlar *et al.* shows the good performances of the M06-2X functional for thermodynamic and kinetic properties,[40] which agrees with our evaluation showing that M06-2X outperforms the B3LYP and BMK functionals[41–43] in comparison with MP2[44] data (ESI†, Section S.1).

Reactions involving large conformational changes such as the rearrangement of water molecules in the solvation shell were analysed with the constrained reduced dimensionality (CRD) method[45] at a lower-level RHF/3-21G* and the located stationary points were later refined at the M06-2X/6-31++G(d,p) level. The STQN method was used for the search of transition states in less complicated cases, and frequency calculations were done at the same computational level M06-2X/6-31++G(d,p) to identify the nature of all optimized stationary points. Changes in Gibbs free energy ($\Delta G$) obtained from these frequency calculations are used for all discussions presented herein.

Solvent effects were included via a self-consistent reaction field (SCRF) in the form of the polarizable continuum model (PCM)[46–48]. The PCM model treats the solvent as a continuum and covers electrostatic solute-solvent interactions well, but it does not include chemical solute-solvent interactions. One or two explicit water molecules were added to the calculations for an accurate description of proton transfer reactions. Water and DMSO were chosen as the main solvents for the analysis. The two solvents have different permittivity (DMSO: 46.826, $H_2O$: 78.3553)[49], but their Clausius Mosotti factors[50] ($cmf = \varepsilon - 1/\varepsilon + 2$) are similar (DMSO: 0.9386, $H_2O$: 0.9627) and hence similar electrostatic solvent effects are expected for them. DMSO and water have the ability to stabilise intermediate zwitterions. The water content of DMSO can be controlled precisely allowing the use of water as a cocatalyst while avoiding large scale hydrolysis and increasing the solubility of the organic reactants simultaneously. The solubility of many organic compounds is significantly higher in alcohols than in pure water. Additional PCM calculations with the geometries optimised for DMSO were done to analyse the influence of methanol, ethanol and 1-propanol on the mechanism of the nornicotine catalysed Mannich reaction.

Experiments[24] show that cyclohexanone and aniline give high yields of the desired Mannich base compared with other possible combinations of reactants; hence, these two compounds were chosen as reactants for the computational analysis. Furthermore, preliminary trial calculations with aniline and formaldehyde using Lehn's equation[31] predict a value of 1.74 for the equilibrium constant for the formation of the imine, *N*-methyleneaniline, in water and that the hydrolysis of the imine does not prevent the formation of the Mannich base. The critical step in the nornicotine catalysed Mannich reaction in water is the formation of the C–C bond between the imine and enamine. The imine can be obtained in a separate step and used as a reactant in its own right. Hence, all energies concerning the Mannich reaction are reported relative to the sum of the energies of the imine, cyclohexanone, and nornicotine for the catalytic reaction.

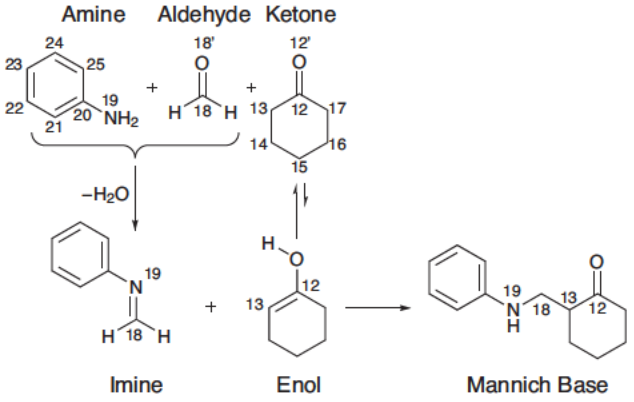


**Scheme 1** The mechanism of the Mannich reaction without a catalyst.

| H+-shuttle \ solvent | DMSO | $H_2O$ | $CH_3OH$ | $C_2H_5OH$ |
|---|---|---|---|---|
| no | 66.398 | 66.638 | — | — |
| 2 $H_2O$ | 41.293 | — | — | — |
| $H_2O$ | 45.590 | 45.659 | 45.513 | 45.436 |
| $CH_3OH$ | — | — | 44.362 | — |
| $C_2H_5OH$ | — | — | — | 44.448 |

**Table 1** Barrier (Gibbs free energy, kcal/mol) for the keto-enol tautomerism (**UC-ts12**) of cyclohexanone in different solvents and with varyious molecules as proton shuttles.

## 3 Results and Discussion

### 3.1 The Mannich Reaction without a Catalyst

The original Mannich reaction (Scheme 1) proceeds in three distinct steps:[1] The amine and the aldehyde form the imine while the ketone tautomerizes into its enol form. The Mannich base is then formed from the products of the two preceding steps.

The rate determining step is the keto-enol tautomerism (Figure 1). The M06-2X/ 6-31++G(d,p) calculations predict its barrier (**UC-ts12**, uncanalysed reaction) in DMSO and water to be 66.40 kcal/mol and 66.64 kcal/mol (Table 1) relative to the solvated cyclohexanone and imine molecules. Both barriers are practically equal to the barrier height of 66.10 kcal/mol reported by da Silva[51] from G3SX[52] calculations in the gas phase. The transition state **UC-ts34** of the C−C bond formation in DMSO is marked by the proton transfer from the enol to the imine with an associated barrier of 32.23 kcal/mol relative to the ketone and the imine. Therefore, the keto-enol tautomerization with the largest barrier is the rate determining step.

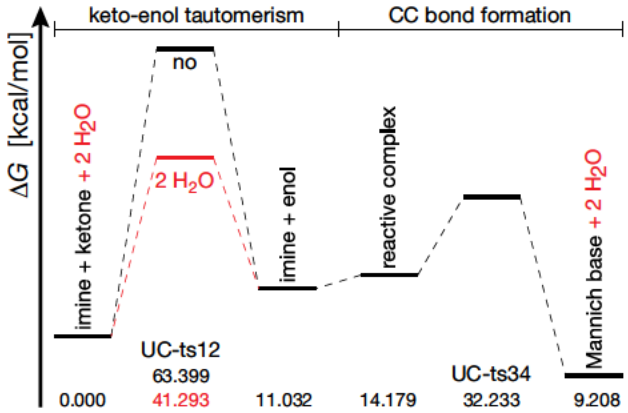


**Fig. 1** Gibbs free energy profile for the uncatalysed Mannich reaction starting form the imine and the ketone. The barrier for the keto-enol tautomerism assisted by two water molecules is given in red for comparison.

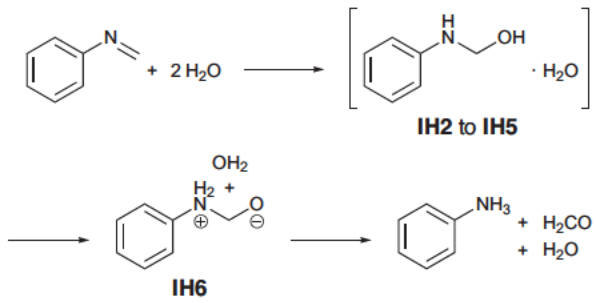


**Scheme 2** Reaction scheme for the imine hydrolysis.

The critical proton transfer in the tautomerization can be accelerated by solvent molecules acting as proton shuttles (Table 1). A single water molecule reduces the barrier significantly by 20.8 kcal/mol in DMSO. The solvent effect for the four solvents, water, DMSO, methanol and ethanol, is negligible and shows that the permittivity of the solvents does not influence the proton shuttle in polar solvents, either. The barrier of the proton transfer is about 1 kcal/mol lower if an alcohol is used both as the solvent and proton shuttle. A larger effect of approximately 4 kcal/mol can be observed, if two water molecules act together to aid the proton transfer. One water molecule accepts the proton from a methylene group while the second water molecule donates a proton to the carbonyl oxygen atom.

### 3.2 Imine Hydrolysis

For simplicity, the imine is regarded as an individual reactant in the Mannich reaction in this report. Starting from this premise, the stability of the imine may potentially become the

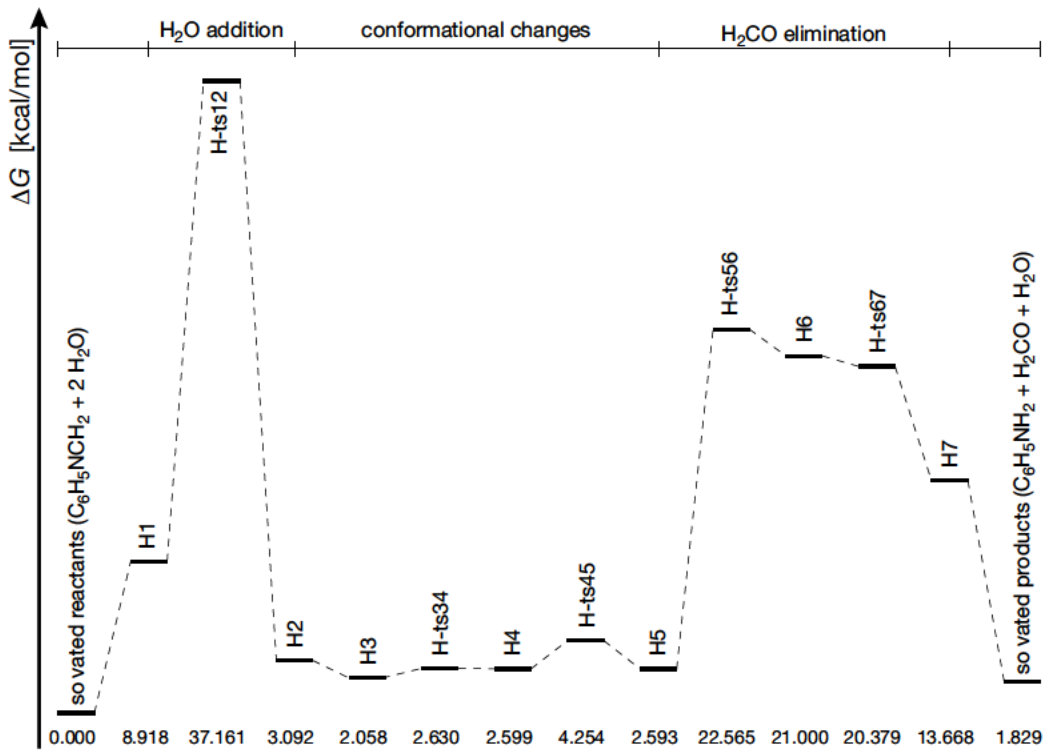


**Fig. 2** Gibbs free energy profile for hydrolysis of the imine in DMSO with two water molecules.

limiting factor for the Mannich reaction in wet solvents or water. A measure for the stability of the imine in water is the equilibrium constant of its formation

$$K_{\text{imine}}^{\text{H}_2\text{O}} = \frac{[\text{imine}]}{[\text{aldehyde}]\,[\text{amine}]} \tag{1}$$

where the square brackets indicate molar concentrations. Lehn *et al.*[31] published an equation

$$\begin{aligned}\log K_{\text{imine}}^{\text{H}_2\text{O}} &= 6.40 \pm 1.62 - (1.04 \pm 0.19)\, E_{\text{LUMO}}^{\text{aldehyde}} \\ &+ (2.00 \pm 0.36)\, E_{\text{HOMO}}^{\text{amine}} + (0.65 \pm 0.07)\, \text{p}K_{\text{A}}^{\text{amine}}\end{aligned} \tag{2}$$

which links the HOMO and LUMO energies of the reactants from B3LYP/6-31G(d,p) calculations and the acid constant of the amine $\text{p}K_{\text{A}}^{\text{amine}}$ to the equilibrium constant $K_{\text{imine}}^{\text{H}_2\text{O}}$ observed in experiments at 25 °C. Setting $E_{\text{LUMO}}^{\text{aldehyde}}$ and $E_{\text{HOMO}}^{\text{amine}}$ equal to −1.172 and −5.391 eV [B3LYP/6-31G(d,p) calculations, this work] and $\text{p}K_{\text{A}}^{\text{amine}}$ to 5.3 yields[31] a value of 0.3 ± 1.7 for $\log K_{\text{imine}}^{\text{H}_2\text{O}}$. Alternatively, the value of $\log K_{\text{imine}}^{\text{H}_2\text{O}}$ directly calculated form the free energies of the reactants and products at the M06-2X/6-31++G(d,p) level with a PCM model for water is 1.3. The estimates obtained by the two methods agree within the methodological uncertainties.

Scheme 2 summarises the mechanism of the imine hydrolysis where the tag **IH** indicates that the molecule/cluster is part of the **i**mine **h**ydrolysis. Figure 2 shows the calculated profile of the Gibbs free energy for the reaction of the imine with two water molecules in DMSO. The rate determine step is the addition of the first water molecule to the imine with the transition state **IH-ts12** with $\Delta G$ equal to 37.161 kcal/mol. The resulting (phenylamino)methanol molecule captures the second water molecule, which will later act as a proton shuttle during the elimination of the formaldehyde molecule. The (phenylamino)methanol-water cluster goes though a series of conformational changes from **IH2** to **IH5** moving the second water molecule into a suitable position to assist the elimination of the formaldehyde molecule. The largest conformational barrier of 4.254 kcal/mol during theses changes has a negligible influence on the overall kinetics of the reaction. A larger barrier of 22.565 kcal/mol in the elimination of the formaldehyde molecule is linked to the transition state **IH-ts56** in which the second water molecule transfers a proton from the OH group to the secondary amino group in the (phenylamino)methanol molecule. The resulting bipolar structure **IH6** readily dissociates into solvated products.

The calculated barriers for **IH-ts12** and **IH-ts56** are 37.153 and 22.563 kcal/mol in water, and 37.161 kcal/mol and 22.565 kcal/mol in DMSO. Apparantly, the permittivity of the solvent only has a small influence on the barrier heights. The importance of the second water molecule as a proton shut-

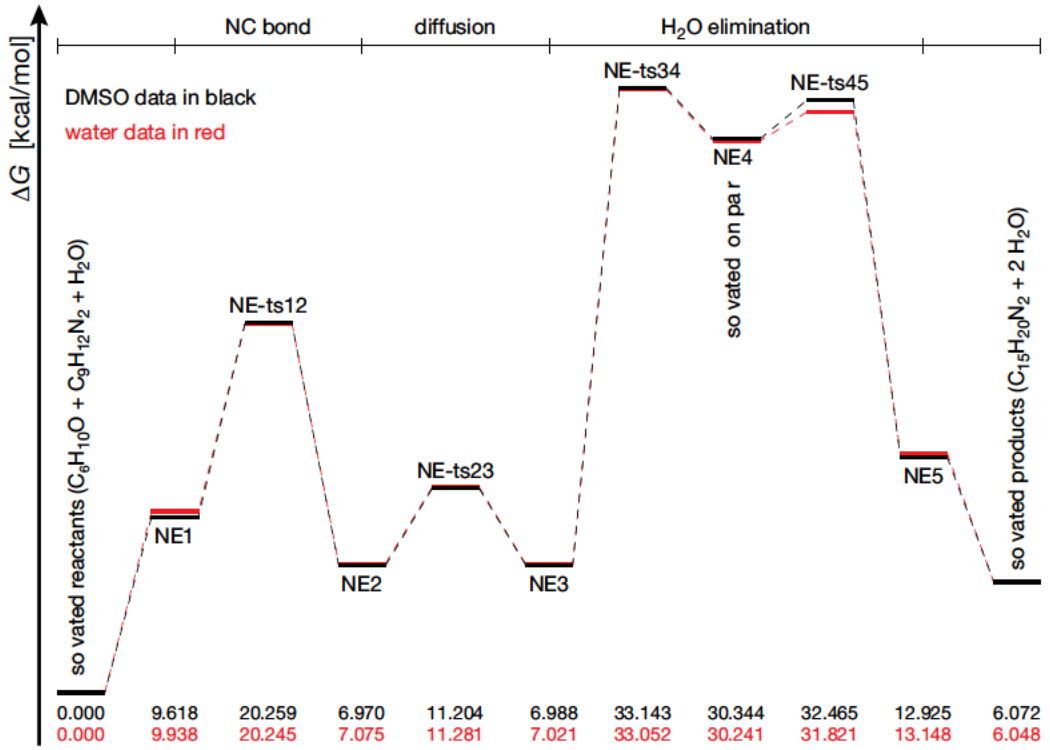


**Fig. 3** The profile of the free energy of the enamine ($C_{15}H_{20}N_2$) formation in DMSO (top, black) and water (bottom, red) relative to that of the solvated reactants cyclohexanone ($C_6H_{10}O$) and nornicotine ($C_9H_{12}N_2$).

tle becomes visible in a simplified simulation of the hydrolysis reaction with a single $H_2O$ molecule in water. The corresponding barriers without a proton shuttle are 51.693 and 36.151 kcal/mol.

In summary, the calculations show that the hydrolysis of the imine to be thermodynamically disfavoured ($\log K_{\text{imine}}^{H_2O} = 1.3$) with a sizable barrier of 37 kcal/mol in the entry channel of the hydrolysis pathway with the aid of two water molecules. An imine, such as *N*-Methyleneaniline, should be able to act as the reactant for the nornicotine catalysed Mannich reaction in wet solvents.

### 3.3 The Nornicotine-catalyzed Mannich Reaction

**3.3.1 Formation of the Enamine.** Scheme 3 shows the mechanism of the water assisted formation of the enamine from nornicotine and cyclohexanone. The corresponding free energy profiles for this reaction in DMSO and water are shown in Figure 3. The five local minima are labelled as **NE1** to **NE5** where the tag **NE** is an abbreviation for **n**ornicotine derived **e**namine. In the first step, the nitrogen atom $N^8$ attacks $C^{12}$, yielding the $N^8$–$C^{12}$ bond while a proton is transferred from $N^8$ to $O^{12'}$ via a water molecule. The water molecule in the product of the first step appears on the side of the pyridine

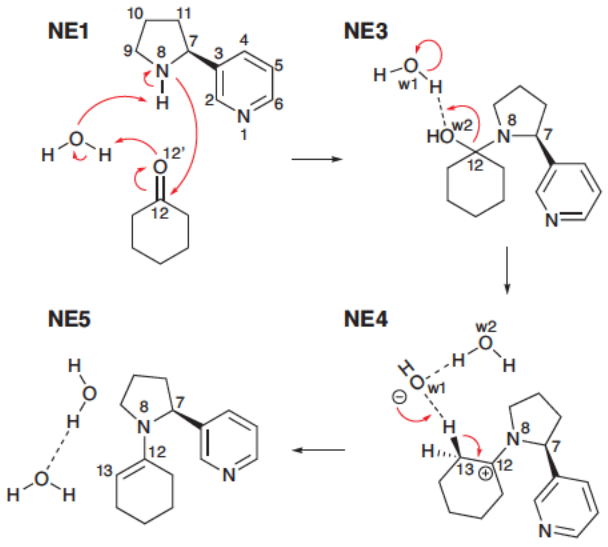


**Scheme 3** The mechanism of formation of the nornicotine-derived enamine. **NE2** and **NE3** are approximately isoenergetic and differ only in the position of the $H_2O$ molecule, as shown in Figure 4.

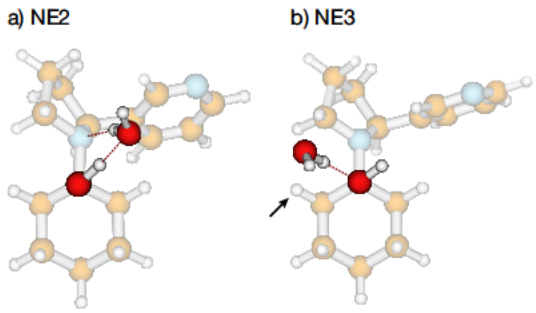


**Fig. 4** Movement of the $H_2O$ molecule between **NE2** and **NE3**. The hydrogen atom to be attacked during the elimination is marked by a small arrow.

ring in **NE2**. Afterwards, it moves to the other side of the $N^8$–$C^{12}$ bond and turns into a hydrogen donor in **NE3**. The complex rotation of the $H_2O$ molecule has a low lying transition state* **NE-ts23** which does not affect the overall speed of the enamine formation. Preliminary molecular dynamics simulations (please refer to the ESI†, Section S.6) show that the water molecule partially detaches from the hydroxy group to move along a curved path to the other side of the $N^8$–$C^{12}$ bond. In an aqueous environment, it is also possible that the process from **NE2** to **NE3** results from an exchange of $H_2O$ molecules with the solvent.

The $H_2O$ elimination appears to proceed via an energetically high lying ion pair **NE4** consisting of an Zundel anion ($H_3O_2^-$) and an carbocation. The positive charge on $C^{12}$ is resonance stabilised by $N^8$ as indicated by the coplanarity of $C^7$, $N^8$, $C^9$, $C^{12}$ and $C^{13}$. In the final step of the enamine formation, the Zundel anion abstracts a proton form $C^{13}$ to yield the enamine adjacent to a water dimer **NE5**. The barrier **NE-ts45** for this step is small compared to the free energy of **NE4**.

The differences in geometry and energy between the PCM calculations for DMSO and water are very small as to be expected from the high permittivity of both solvents[53] ($\varepsilon_{DMSO}$ = 46.8, $\varepsilon_{H_2O}$ = 78.4). The largest difference in free energy is the transition state for the destruction of the ion pair **NE-ts45** with a difference $\Delta\Delta G^{\ddagger}$ of 0.644 kcal/mol. However, this difference is so small that the two free energy profiles for the formation of the enamine can be regarded as practically identical. More importantly, the free energy of **NE-ts34** which is 33.143 kcal/mol and 33.052 kcal/mol relative to the solvated reactants in DMSO and $H_2O$ is significantly lower than the smallest barrier for the keto-enol tautomerism 41.293 kcal/mol; hence the formation of the nornicotine derived enamine is clearly preferred to the tautomerisation of cyclohexanone. The free energy 33.143 kcal/mol of **NE-ts34** is also smaller than 37.161 kcal/mol of **IH-ts12**. It is concluded that the formation of enamine is kinetically preferred to the hydrolysis of the imine.

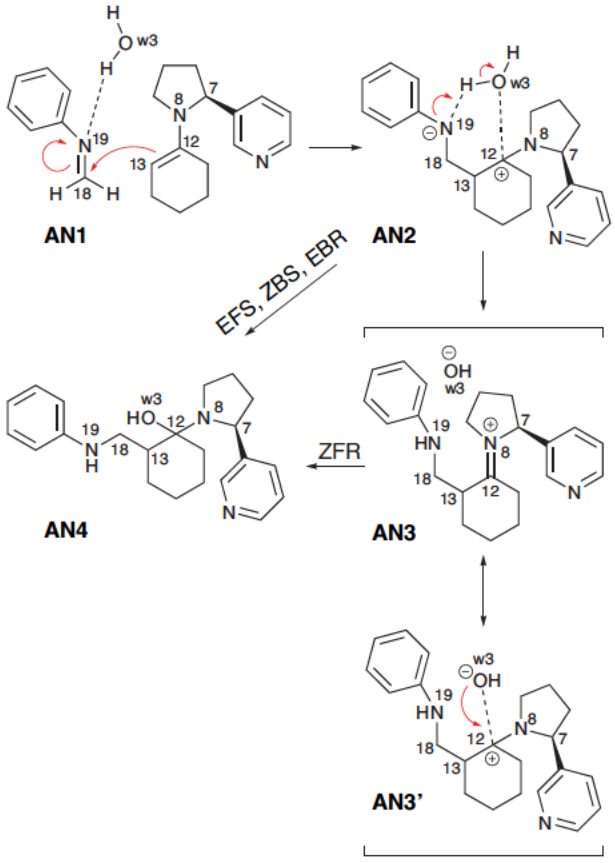


**Scheme 4** The mechanism of formation of the aminol.

**3.3.2 Formation of the Aminol.** The enamine can react with the imine starting from the reactive cluster **AN1** to yield an aminol **AN4**, which is the precursor of the desired Mannich base, as illustrated in Scheme 4. During this process, the $C^{12}$=$C^{13}$ double bond and the pyridine ring can either be on the same side (*Z*-rotamer) or on opposite sides (*E*-rotamer) of the enamine. The largest barrier in the path between these two rotamers is 8.73 kcal/mol in DMSO (ESI†, Section S.2), indicating a rapid conversion between them. In both rotamers, the imine molecule can attack $C^{13}$ either from the side of the pyridine ring (F, front) or from the opposite side (B, back). The four possible routes to the aminol **AN4** are summarized in Figure 5, namely EBR, EFS, ZFR, and ZBS.

**AN4** is formed in two distinct steps of which the $C^{13}$–$C^{18}$ bond and the new chiral center on $C^{13}$ are formed in the first

* The DMSO-geometry of **NE-ts23** was not reoptimized in PCM-water, because the initial frequency calculation with DSMO-geometry in water yield one and only one imaginary frequency which is linked to the reaction coordinate of the water rotation.

| | | AN1 | AN-ts12 | AN2 | AN3 | AN-ts34 | AN4 |
|---|---|---|---|---|---|---|---|
| Mulliken | $N^8$ | 0.0246 | 0.2010 | 0.2669 | 0.3251 | 0.3769 | 0.1358 |
| | $C^{12}$ | −0.7216 | −0.1865 | −0.4099 | −0.3385 | −0.8300 | −0.2542 |
| | $N^{19}$ | −0.3103 | −0.2622 | −0.4679 | −0.4329 | −0.2692 | −0.1818 |
| APT charge | $N^8$ | −1.1568 | −0.8648 | −0.7095 | −0.7004 | −0.9542 | −0.9557 |
| | $C^{12}$ | 0.6879 | 0.8457 | 0.7524 | 0.7223 | 1.2224 | 0.9965 |
| | $N^{19}$ | −0.7612 | −1.7248 | −1.7222 | −1.6171 | −1.3737 | −1.0876 |

**Table 2** Selected Mulliken and APT charges along ZBS route in DMSO. Charges in multiples of *e*.

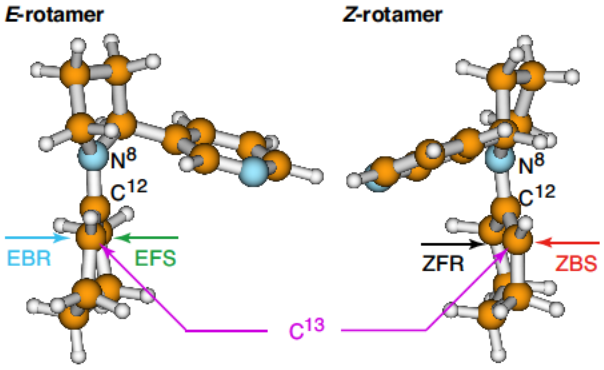


**Fig. 5** The four routes from **AN1** to **AN4**. The three characters indicate the enamine rotamer (Z or E), the direction of the attack (F or B) and the resulting absolute configuration of $C^{13}$ (S or R). $C^{13}$ is the closest to the observer in both plots.

step. Table 2 list the charge of selected atoms obtained by Mulliken and APT population analyses during the formation of the aminol along the path with the lowest barrier. The charge on $N^{19}$ becomes more negative as the reaction proceeds form **AN1** to **AN2** while $C^{12}$ becomes more positive or less negative. Both charge analyses rule out an alternative scenario in which electron density flows from the imine to the enamine since such a flow would lead to different signs for the charges on $N^8$ and $N^{19}$. The resulting bipolar structure in **AN2** is stabilised by the water molecule **w3** bridging the gap between $C^{12}$ and $N^{19}$.

The formations of the $N^{19}$–H and the $C^{12}$–$O^{w3}$ bonds are not correlated as the $N^{19}$–H bond readily forms at the beginning of the following step while the addition of $O^{w3}$ to $C^{12}$ can be sterically hindered. This hinderance in the formation of the $C^{12}$–$O^{w3}$ bond enables the barrierless formation of an intermediate ion pair **AN3**. The energy of **AN2** increases continuously as the hydroxide ion is formed and finally levels at lower values than that for the transition state in the formation of the $C^{12}$–$O^{w3}$ bond. In three of the four analysed cases (EFS, ZBS, EBR) the transition state for the formation of the $C^{12}$–$O^{w3}$ bond starting from the ion pair **AN3** coincides with that starting from **AN2** so that **AN-ts34** and **AN-ts24** are the same point on the potential energy surface of the formation of the aminol. Hence, the formation the intermediate ion pair **AN3** can be regarded as a simple detour. However, in ZFR, the formation of **AN4** from **AN3/AN3'** has been found to be barrierless and hence the energy of the intermediate ion pair **AN3** is taken as the effective barrier of 22.91 kcal/mol for the formation of **AN4** from **AN2**. The barrier **AN-ts24** for the formation of **AN4** in a single step from **AN2** is 27.293 kcal/mol in DMSO (Table 3) which shows that the formation of the aminol **AN4** proceeds *via* **AN3** along ZFR path.

The proton movement from $O^{w3}$ to $N^{19}$ reduces the negative charge on $N^{19}$ and yields a hydroxide ion. The Mulliken analysis suggests that the positive charge on $N^8$ increases during the proton movement. The APT analysis supports such a change in polarity; though to a much smaller extent. However, the two charge analyses disagree on the polarity of the $C^{12}$=$N^8$ bond. The Mulliken charge analysis places the positive charge on $N^8$ whereas the APT analysis puts it on $C^{12}$. **AN3** and **AN3'** are shown as resonant structures in Scheme 4. The APT analysis supports the observed addition of the $OH^-$ ion to $C^{12}$ while the Mulliken analysis indicates the stabilisation of the positive charge on $C^{12}$ by the lone pair electrons on $N^8$. This assumption is further supported by the shortening of the $N^8$–$C^{12}$ bond from 1.392 Å in **AN1** to 1.293 Å in **AN3** and the planar structure of the link as indicated by the small $C^7N^8C^{12}C^{13}$ dihedral angles of −1.2° and −3.4° respectively.

The *S*-aminol is formed by a front-side attack on the *E*-conformer (EFS) and a back-side attack on the *Z*-conformer (ZBS) while the *R*-aminol is formed along the other twopathways (EBR and ZFR). The free energies of the stationary points along the reaction path from **AN1** to **AN4** are listed in Table 3. The reactive complexes leading to the *S*-product are generally more stable than those leading to the *R*-product. The direct products from a frontside attack are preferred to those

| path | solvent | AN1 | AN-ts12 | AN2 | AN3 | AN-ts34 | AN-ts24 | AN4 |
|---|---|---|---|---|---|---|---|---|
| EFS | DMSO | 10.276 | 24.458 | 20.241 | 22.786 | 34.354 | 34.354 | -3.473 |
| ZBS | DMSO | 12.312 | 24.450 | 17.870 | 19.842 | 25.889 | 25.889 | 2.858 |
| EBR | DMSO | 13.296 | 25.337 | 20.525 | 22.214 | 26.242 | 26.424 | 0.024 |
| ZFR | DMSO | 13.262 | 30.309 | 22.232 | 22.910 | — | 27.293[(1)] | -2.606 |
| EFS | $H_2O$ | 10.317 | 24.432 | 20.104 | 22.467 | 34.171 | 34.171 | -3.387 |
| ZBS | $H_2O$ | 12.301 | 24.491 | 17.834 | 19.779 | 25.988 | 25.988 | 2.912 |
| EBR | $H_2O$ | 13.372 | 25.326 | 20.477 | 22.325 | 26.155 | 26.155 | 0.083 |
| ZFR | $H_2O$ | 13.388 | 30.521 | 22.057 | 22.723 | — | 27.112[(1)] | -2.480 |

**Table 3** Free energies in kcal/mol of the stationary points shown in Scheme 4 relative to that of the solvated reactants. The rate determining barriers are marked in red. The transition states for the EFS, ZBS, EBR reactions starting either at **AN2** or **AN3** are identical. [(1)]Geometries localised with the CRD algorithm[45] and optimised at the M06-2X/6-31G(d) with a PCM model for DMSO followed by M06-2X/6-31++G(d,p) single point calculations either in DMSO or in water.

from a backside attack, while the most stable intermediates both **AN2** and **AN3** are observed during a backside attack.

The kinetics of the formation of the aminol **AN4** are controlled by two barriers **AN-ts12** and **AN-ts34** of similar size. The exit-barrier **AN-ts34** is the rate determining barrier along the three paths EFS, ZBS and EBR. Despite of all attempts on a comprehensive search, no transition state **AN-ts34** was found for the third step of the ZFR path which indicates a barrier-free addition of the hydroxide ion to the carbocation in **AN3** along the ZFR path, consequently the formation of the CC bond in **AN-ts12** is the rate determining step along the ZFR path.

The lowest barrier for a rate determining step of 25.889 kcal/mol (**A-ts34**) is found along the ZBS path which suggests that the *S*-aminol to be the dominating product. The second lowest barrier of 26.242 kcal/mol is observed along the EBR path. The barriers along the EFS and ZFR path are so high that these two paths are not expected to participate in the overall formation of the aminol. The free energy difference between **AN-ts34** along the ZBS and EBR paths derives an enantiomeric excess of 29% ee of the *S*-aminol in DMSO.[54,55] The difference in free energy between the *Z*- and *E*-rotamers of the product **AN4** is much larger than that between the reactants **AN1**. The aforementioned small barrier for the rotation around the $C^{12}$–$N^8$ bond in the enamine indicate that thermal equilibration will favour the *E*-rotamer for the S-product and *Z*-rotamer for the R-product.

The data in Table 3 show that a change of solvent from DMSO to water will only have a small influence on the formation of the aminol. The largest solvent effect of −0.614 kcal/mol is observed for **AN-ts23** where the higher permittivity of water facilitates the formation of the ion pair **AN3**. The free energy of **AN-ts34** is 0.099 kcal/mol higher along the ZBS path and 0.087 kcal/mol lower along the EBR pathway in water than in DMSO. These changes reduce the difference in barrier height for the rate determining steps; thus a smaller enantiomer excess of 14% ee is observed for water.

Although nornicotine and proline have the pyrrolidine ring in common, proline is strongly stereoselective while the current analysis yield only a small effect for nornicotine. Similar values of about 20% ee have been reported for the stereoselectivity of the nornicotine catalyzed aldol reaction.[17]

**3.3.3 Release of the Nornicotine Catalyst.** The Mannich base is finally formed in the dissociation of the aminol **AN4**. Scheme 5 summarises the mechanism of the hydrolysis of the aminol with and without a catalytic water molecule. The water molecule **w4** acts as a proton shuttle in the case of water catalysis similar to the mechanism discussed by Janda *et al.*[28] for the water based aldol reaction. Figure 6 shows the profile for the relative free energy for the water catalysed release of the Mannich base form the ZBS- and the EBR-aminol. The barriers in the range of 20 to 26 kcal/mol for the proton transfer are comparable to those for the aminol formation (Table 3). Therefore, the formation of the enamine with a barrier of 33.143 and 33.052 kcal/mol (Figure 3) in DMSO and water is the rate determining step.

The catalytic effect of water becomes evident by the comparison of the uncatalysed reaction (Scheme 5b) with the water catalysed one for the EBR-aminol. The barriers for the proton transfer from the hydroxyl group to $N^8$ in DMSO and water are 33.807 and 33.814 kcal/mol which on average are 13.7 kcal/mol higher than those in the case of the catalysed reaction. The close similarity of the barriers for the uncatalysed reaction in water and DMSO in contrast to the catalytic

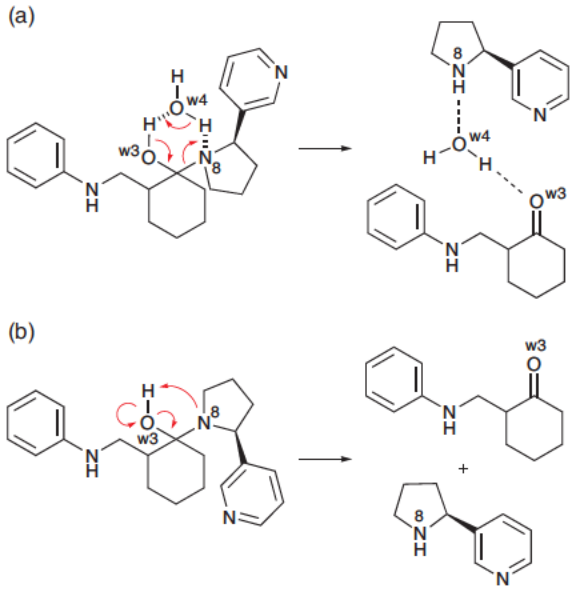


**Scheme 5** The release of the Mannich base and nornicotine from **AN4**. a) Assisted by a water molecule. b) Without a water assistance.

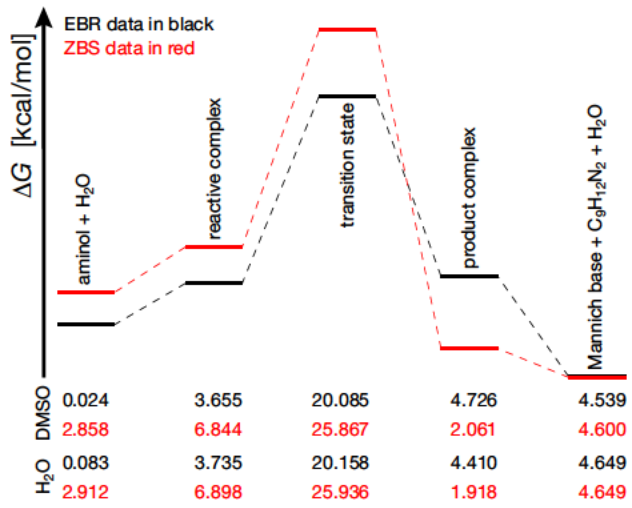


**Fig. 6** Relative free energy during the formation of the Mannich base from the aminol and the release of the nornicotine catalysts $C_9H_{12}N_2$. All energies are given in kcal/mol.

effect highlights once more the importance of explicit solute-solvent interactions. Hence, catalytic amounts of water in the solvent are crucial for the nornicotine catalysis of the Mannich reaction.

### 3.4 Other solvents

The addition of alcohols to water can increase the solubility of the organic reactants so significantly that the speed of the nornicotine catalysed reaction is enhanced. Table 4 lists the results for the rate determining barriers in different solvents. All calculations were done with the geometries obtained from the geometry optimisations in DMSO including the water molecules necessary for the proton transfer. The frequency calculations with these geometries yielded one and only one imaginary frequencies for the transition states and all real for the local minima (please refer to the ESI† Section S.5 for details).

The reduction of the solvent's permittivity increases the barrier for the formation of the enamine (**NE-ts34**), which is the rate determining step in all solvents. A comparison with the data in Table 1 for the keto-enol equilibrium further indicates that a sizeable catalytic effect should exist in methanol and ethanol, too. On the other hand, an exchange of the solvent shows only a minor influence on the equilibrium between the Mannich base and the reactants, imine and cyclehexanone. On average, the calculations yield an equilibrium constant of $2.4 \times 10^3$ for the formation of the Mannich base.

The barrier heights for the formation of the *S*- and *R*-aminol are nearly unaffected by the changes in the PCM solvent and hence similar values for enantiomeric access are observed for the five solvents. This observation agrees with those listed in Table 3 where the optimisation of the corresponding transition states also yielded only very small changes in the free energies. In summary, the data in Tables 3 and 4 lead to the conclusion that the addition of alcohols to the solvent is likely to slightly increase the enantiomeric excess; however; it is remarked that the prediction of the extend of this increases is not quantitatively precise with the computational approach and model used.

## 4 Conclusions

The DFT calculations with the approximate treatment of solvents as polarizable continuums show that nornicotine forms water stable enamines which can substitute the enol in Mannich reactions. The stability of nornicotine derived enamines in water is well established [17,29] which makes the stability of the intermediate imine crucial for the success of water based Mannich reaction. The rate determining barrier for the hydrolysis of the imine *N*-methyleneaniline is 37.16 kcal/mol (Figure 2) which is 11 kcal/mol higher than the barrier for the formation of the aminol along the ZBS path (Tabble 3). Therefore, the formation of the Mannich base is much more likely than the hydrolysis of the imine. It is also 4.1 kcal/mol higher than the barrier for the formation of the enamine from nornicotine and cyclohexanone which suggests that a steady

| | $H_2O$[a] | DMSO | $CH_3OH$[a] | $C_2H_5OH$[a] | $n$-$C_3H_7OH$[a] |
|---|---|---|---|---|---|
| permittivity[b] $\varepsilon$ | 78.3553 | 46.826 | 32.613 | 24.852 | 20.493 |
| $(\varepsilon-1)/(\varepsilon+1)$ | 0.9627 | 0.9386 | 0.9133 | 0.8883 | 0.8668 |
| enamine | 33.112 | 33.143 | 33.173 | 33.202 | 33.226 |
| aminol - ZBS | 25.894 | 25.889 | 25.885 | 25.882 | 25.880 |
| aminol - EBR | 26.243 | 26.242 | 26.242 | 26.247 | 26.226 |
| excess % ee | 28.7 | 29.0 | 29.3 | 29.8 | 28.4 |
| product - ZBS | 25.917 | 25.867 | 25.806 | 25.745 | 25.692 |
| product - EBR | 20.137 | 20.085 | 20.027 | 19.968 | 19.915 |
| Mannich base | −4.588 | −4.539 | −4.631 | −4.635 | −4.646 |
| $K$[c] | $2.3 \times 10^3$ | $2.1 \times 10^3$ | $2.5 \times 10^3$ | $2.5 \times 10^3$ | $2.5 \times 10^3$ |

**Table 4** Comparison of the barrier heights in kcal/mol relative to the solvated reactants in various solvents. [a] Geometries optimised in DMSO. [b] Permittivity data taken from the Gaussian 09 webpage. [c] Equilibrium constant $K$ for the formation of the Mannich base from the imine and cyclohexanone.

enamine supply will prevent a rapid hydrolysis of the imine. Furthermore, the usage of imines more stable in water than *N*-methyleneaniline[31] is likely to increase the overall yield of the targeted Mannich base.

The rate determining step for the catalytic process is the formation of the enamine in the studied solvents. It is about 12 kcal/mol lower than that for the keto-enol tautomerism of the uncatalysed Mannich reaction; hence, a substantial catalytic effect ought to be expected with nornicotine in water, DMSO and small alcohols. The calculated values of $\Delta G$ for the formation of the Mannich base from *N*-methyleneaniline and cyclohexanone are −4.57 kcal/mol in DMSO and −4.65 kcal/mol in water such that the solvent seems to have only a small influence on the position of the equilibrium ($K \approx 2.4 \times 10^3$). Nornicotine catalysis appears to be kinetically and thermodynamically feasible.

Nornicotine is part of the natural chiral pool and the chiral center on $C^2$ of the pyrollidine ring is expected to exert stereochemical control over the formation of the Mannich base. The calculated enantiomeric excesses of the *S*-Mannich base of 29 and 14% ee in DMSO and water are comparable to known data for the nornicotine catalysis of the aldol reaction.[17]

This study suggests that the successful formation of Mannich bases should be possible in water. If a low solubility of the reactants in water or simple alcohols should make the use of non-polar organic solvents necessary, it is suggested that small amounts of water should be added as a cocatalyst, because water molecules are an indispensable part of the catalytic process.

In summary, it has been shown that nornicotine catalysis can replace hazardous organic solvents by water in the synthesis of Mannich bases. At a bare minimum, nornicotine catalysis would remove the need of dry solvents form synthesis. The authors hope that the present study will lead to green versions of the Mannich reaction with a reduced environmental impact.

## 5 Acknowledgement

This work is supported by the National Science Council of Taiwan (R.O.C.) under Grant NSC 100-2113-M-007-008-MY3. T.L. acknowledges a university research associateship from the National Tsing Hua University.

## References

1 M. Arend, B. Westermann and N. Risch, *Angew. Chem. Int. Ed.*, 1998, **37**, 1044–1070.
2 S. G. Pyne, C. W. G. Au, A. S. Davis, I. R. Morgan, T. Ritthiwigrom and A. Yazici, *Pure Appl. Chem.*, 2008, **80**, 751–762.
3 N. Risch and A. Esser, *Liebigs. Ann. Chem.*, 1992, **1992**, 233–237.
4 B. List, P. Pojarliev, W. T. Biller and H. J. Martin, *J. Am. Chem. Soc.*, 2002, **124**, 827–833.
5 M.-O. Simon and C.-J. Li, *Chem. Soc. Rev.*, 2012, **41**, 1415–1427.
6 U. M. Lindström, *Chem. Rev.*, 2002, **102**, 2751–2772.
7 J. Paradowska, M. Stodulski and J. Mlynarski, *Angew. Chem. Int. Ed.*, 2009, **48**, 4288–4297.
8 M. Rogozińska, A. Adamkiewicz and J. Mlynarski, *Green Chem.*, 2011, **13**, 1155–1157.
9 R. L. Chelvarajan, F. F. Fannin and L. P. Bush, *J. Agric. Food Chem.*, 1993, **41**, 858–882.
10 B. Siminszky, L. Gavilano, S. W. Bowen and R. E. Dewey, *Proc. Nat. Acad. Sci. U.S.A.*, 2005, **102**, 14919–14924.
11 T. Bartholomeusz, R. Bhogal, R. Molinié, F. Felpin, M. Mathé-Allainmat, A. Meier, B. Dräger, J. Lebreton, A. Roscher, R. Robins and F. Mesnard, *Phytochemistry*, 2005, **66**, 2432–2440.

12 B. Liu, C. Chen, D. Wu and Q. Su, *J. Chromatogr. B*, 2008, **865**, 13–17.
13 T. J. Dickerson and K. D. Janda, *Proc. Natl. Acad. Sci. U.S.A.*, 2002, **99**, 15084–15088.
14 J. B. Treweek, T. J. Dickerson and K. D. Janda, *Acc. Chem. Res.*, 2009, **42**, 659–669.
15 T. J. Dickerson and K. D. Janda, *J. Am. Chem. Soc.*, 2002, **124**, 3320–3321.
16 T. J. Dickerson and K. D. Janda, *Proc. Natl. Acad. Sci. U.S.A.*, 2003, **100**, 8182–8187.
17 A. P. Brogan, T. J. Dickerson and K. D. Janda, *Angew. Chem. Int. Ed.*, 2006, **45**, 8100–8102.
18 C. Schöpf, *Angew. Chem.*, 1937, **50**, 779–787.
19 C. Schöpf, *Angew. Chem.*, 1937, **50**, 797–805.
20 V. Vinković and V. Sunjić, *Tetrahedron*, 1997, **53**, 689–696.
21 C. F. B. Armando Córdova, *Tetrahedron Lett.*, 2003, **44**, 1923–1926.
22 A. Córdova, *Acc. Chem. Res.*, 2004, **37**, 102–112.
23 I. Ibrahem and A. Córdova, *Chem. Comm.*, 2006, 1760–1762.
24 I. Ibrahem, W. Zou, J. Casas, H. Sundén and A. Córdova, *Tetrahedron*, 2006, **62**, 357–364.
25 L. Cheng, X. Wua and Y. Lu, *Org. Biomol. Chem.*, 2007, **5**, 1018–1020.
26 Y. Hayashi, T. Urushima, S. A. abd Tsubasa Okano and K. Obi, *Org. Lett.*, 2007, **10**, 2124.
27 N. Mase and C. F. Barbas, III, *Org. Biomol. Chem.*, 210, **8**, 4043–4050.
28 T. J. Dickerson, T. Lovell, M. M. Meijler, L. Noodleman and K. D. Janda, *J. Org. Chem.*, 2004, **69**, 6603–6609.
29 C. J. Rogers, T. J. Dickerson and K. D. Janda, *J. Org. Chem.*, 2005, **70**, 3705–3708.
30 C. J. Rogers, T. J. Dickerson and K. D. Janda, *Tetrahedron*, 2006, **62**, 352–356.
31 C. Godoy-Alcántar, A. K. Yatsimirsky and J.-M. Lehn, *J. Phys. Org. Chem.*, 2005, **18**, 979–985.
32 K. Meguellati, A. Fallah-Araghi, J.-C. Baret, A. E. Harrak, T. Mangeat, C. M. Marques, A. D. Griffiths and S. Ladame, *Chem. Comm.*, 2013, 11332–11334.
33 *U.S. National Library of Medicine: Nornicotine*, visited March 31, 2014, `http://chem.sis.nlm.nih.gov/chemidplus/rn/494-97-3`.
34 M. J. Frisch *et al.*, *Gaussian 09 Revision A.1*, Gaussian Inc. Wallingford CT 2009 (see ESI† for complete reference).
35 Y. Zhao and D. G. Truhlar, *Theor. Chem. Acc.*, 2008, **120**, 215–241.
36 R. Ditchfield, W. J. Hehre and J. A. Pople, *J. Chem. Phys.*, 1971, **54**, 724–728.
37 M. M. Francl, W. J. Pietro1, W. J. Hehre, J. S. Binkley, M. S. Gordon, D. J. DeFrees and J. A. Pople, *J. Chem. Phys.*, 1982, **77**, 3654–3665.
38 T. Clark, J. Chandrasekhar, G. W. Spitznagel and P. V. R. Schleyer, *J. Comp. Chem.*, 1983, **4**, 294–301.
39 M. J. Frisch, J. A. Pople and J. S. Binkley, *J. Chem. Phys.*, 1984, **80**, 3265–3269.
40 Y. Zhao and D. G. Truhlar, *Acc. Chem. Res.*, 2008, **41**, 157–167.
41 A. D. Becke, *J. Chem. Phys.*, 1993, **98**, 1372–1377.
42 C. Lee, W. Yang and R. G. Parr, *Phys. Rev. B*, 1988, **37**, 785–789.
43 A. D. Bose and J. M. L. Martin, *J. Chem. Phys.*, 2004, **121**, 3405–3416.
44 C. Møller and M. S. Plesset, *Phys. Rev.*, 1934, **46**, 618–622.
45 T. Lankau and C.-H. Yu, *J. Chem. Phys.*, 2013, **138**, 214102.
46 S. Miertuš, E. Scrocco and J. Tomasi, *Chem. Phys.*, 1981, **55**, 117–129.
47 E. Cancès, B. Mennucci and J. Tomasi, *J. Chem. Phys.*, 1997, **107**, 3032–3041.
48 G. Scalmani and M. J. Frisch, *J. Chem. Phys.*, 2010, **132**, 114110.
49 Gaussian Official webpage;, *G09 Keyword: SCRF;*, `http://www.gaussian.com/g_tech/g_ur/k_scrf.htm`, visited 22.10.2013.
50 P. V. Rysselberghe, *J. Phys. Chem.*, 1932, **36**, 1152–1155.
51 G. da Silva, *Angew. Chem., Int. Ed.*, 2010, **49**, 7685–7687.
52 L. A. Curtiss, P. C. Redfern1, K. Raghavachari and J. A. Pople, *J. Chem. Phys.*, 2001, **114**, 108–117.
53 *G09 Keyword: SCRF*, visited October 25, 2012, `http://www.gaussian.com/g_tech/g_ur/k_scrf.htm`.
54 N. S. Zefirov, *Tetrahedron*, 1977, **33**, 2719–2722.
55 H. Maskill, *The Physical Basis of Organic Chemistry*, Oxford University Press, Oxford, UK, 1989.

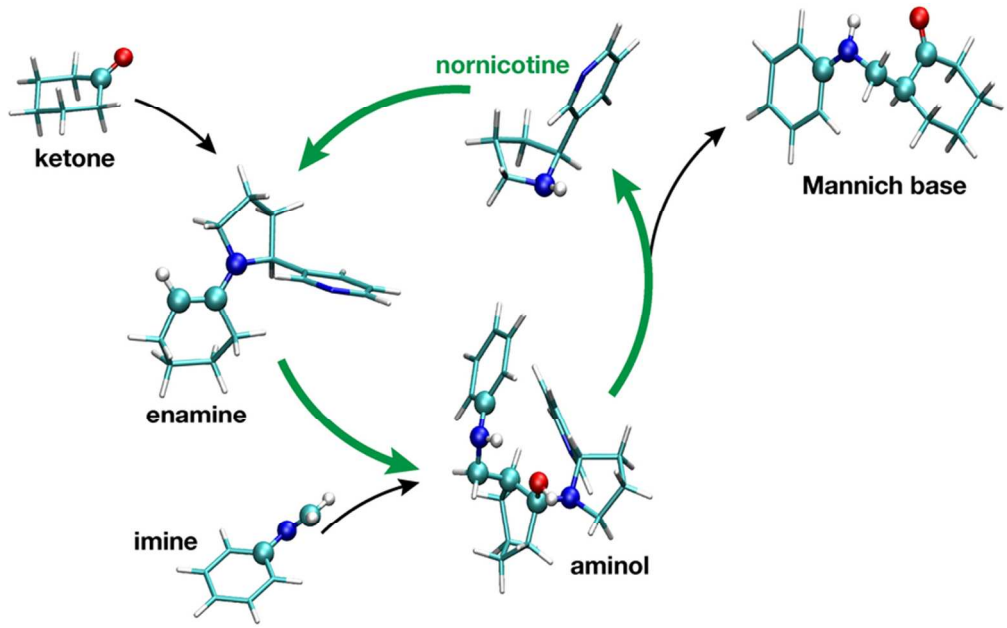


Quantum calculations lead the way to a green version of the versatile Mannich reaction in water catalysed by nornicotine.
40x24mm (600 x 600 DPI)

# A Theoretical Study of the Nornicotine-Catalyzed Mannich Reaction in Wet Solvents and Water

Sheng-Che Yang‡
Department of Chemistry, National Tsing Hua University
101 KuangFu Road Sec.2, Hsinchu 30013, Taiwan
e-mail: jetyaung@gmail.com

Timm Lankau‡
Department of Chemistry, National Tsing Hua University
101 KuangFu Road Sec.2, Hsinchu 30013, Taiwan
e-mail: lankau@oxygen.chem.nthu.edu.tw
phone: (+)886-3-5715131-33414 fax: (+)886-3-5711082

Chin-Hui Yu (corresponding author)
Department of Chemistry, National Tsing Hua University
101 KuangFu Road Sec.2, Hsinchu 30013, Taiwan
e-mail: chyu@oxygen.chem.nthu.edu.tw
phone: (+)886-3-5162080 fax: (+)886-3-5711082

‡ These authors contributed equally to this work.

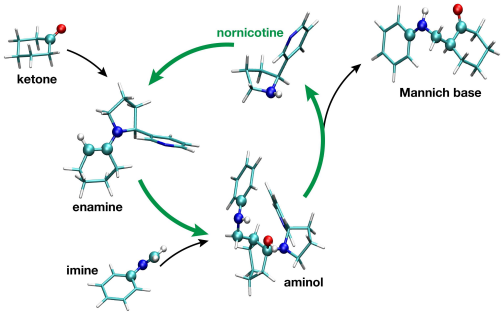


Quantum calculations lead the way to a green version of the versatile Mannich reaction in water catalysed by nornicotine.

Keywords: Nornicotine, DFT, Catalysis, Water as solvent, Mannich reaction